DALTON
FULL PAPER

Synthesis, characterisation and electrochemical reductions of oxo-centred, carboxylate-bridged triiron complexes, $[Fe_3(\mu_3\text{-}O)(\mu\text{-}O_2CR)_6L_3]X$ (R = Me, Bu^t, Ph, CH_2Cl, CCl_3, CH_2CN or 4-$NO_2C_6H_4$; L = py, 3-H_2Npy, 4-H_2Npy, 3-NCpy, 4-NCpy or 4-CH_2CHpy; X = ClO_4^- or NO_3^-)

Alan M. Bond,[a] Robin J. H. Clark,*[,b] David G. Humphrey,*[,a,b] Paris Panayiotopoulos,[b] Brian W. Skelton[c] and Allan H. White[c]

[a] *Department of Chemistry, Monash University, Wellington Road, Clayton, Victoria 3168, Australia*
[b] *Christopher Ingold Laboratories, University College London, 20 Gordon Street, London, UK WC1H 0AJ*
[c] *Department of Chemistry, University of Western Australia, Nedlands, Western Australia, 6907, Australia*

A range of oxo-centred, carboxylate-bridged triiron complexes of general formula $[Fe_3O(O_2CMe)_6L_3]X$ (L = py, 3-H_2Npy, 4-H_2Npy, 3-NCpy, 4-NCpy or 4-CH_2CHpy, X = ClO_4^-) and $[Fe_3O(O_2CR)_6(py)_3]X$ (R = Bu^t, Ph, CH_2Cl, CCl_3, CH_2CN or 4-$NO_2C_6H_4$, X = ClO_4^- or NO_3^-) has been synthesized, some for the first time. The $[Fe_3O(O_2CPh)_6(py)_3]NO_3$ complex (as its dichloromethane solvate) has been the subject of a room-temperature single-crystal X-ray study. The redox behaviour of these complexes has been investigated by cyclic voltammetry in 0.2 mol dm^{-3} $[NBu_4][PF_6]$–dichloromethane, in the presence and absence of free L (where L is pyridine or substituted pyridine). These complexes in general display a chemically reversible one-electron reduction to the neutral mixed-valence species at +0.5 to −0.2 V, *vs.* Ag–AgCl, provided an excess of free L is present. The reversible potential of the $[Fe_3O(O_2CMe)_6L_3]^{+/0}$ and $[Fe_3O(O_2CR)_6(py)_3]^{+/0}$ reductions varies linearly with the pK_a of L and ^-O_2CR. A second reduction was also detected at more negative potentials. Only for R = CH_2CN the second reduction becomes chemically reversible in the presence of free pyridine, such that the monoanion, $[Fe_3O(O_2CR)_6(py)_3]^-$, is stable on the timescale of the voltammetric experiment. Where solubility and stability permitted, the $[Fe_3O(O_2CMe)_6L_3]$ and $[Fe_3O(O_2CR)_6(py)_3]$ complexes have been electrogenerated *in situ*. The mixed-valence species display an extremely broad, low intensity ($\varepsilon \approx 60$–100 dm^3 mol^{-1} cm^{-1}) band in the 7000–8000 cm^{-1} region of the electronic spectrum.

Oxo-centred, carboxylate-bridged trinuclear complexes of general formula $[M_3(\mu_3\text{-}O)(O_2CR)_6L_3]^{z+}$ are known for a number of transitional-metal ions.[1–3] Complexes of this structure contain a triangular arrangement of metal ions bridged by a central oxo group. The carboxylate anions each span two metal centres about the periphery of the $\{M_3(\mu_3\text{-}O)\}^{z+}$ core, whilst the neutral unidentate ligands occupy the remaining co-ordination sites on each metal centre (*trans* to the bridging oxo ligand), such that the geometry about each metal centre is approximately octahedral. For the case where M = Fe, $[Fe_3O(O_2CR)_6L_3]^z$ complexes have been isolated in two oxidation levels, *viz.* the monocationic species ($z = 1+$) and the neutral mixed-valence complex ($z = 0$).[1] The triangular oxo-centred structure was confirmed in 1965 and, since then,[4] attention has focused almost exclusively on various properties of these complexes in the solid state.[5,6] The highly symmetrical structure and the relatively large metal–metal distances, which exclude the possibility of direct metal–metal bonding, make these attractive systems with which to examine magnetic and electronic interactions. The monocationic complexes, which contain three high-spin iron(III) centres, were some of the first polynuclear systems to which ideas of magnetic exchange were applied,[7] whilst the neutral complexes display intriguing temperature-dependent mixed-valence behaviour and have been examined by many physical techniques.[5] These studies and numerous others have addressed various aspects of the chemistry of these systems in the solid state, whilst the solution properties of these complexes remain comparatively less well explored.[8] In order to extend the solution chemistry of the triiron systems, a series of $[Fe_3O(O_2CMe)_6L_3]X$ and $[Fe_3O(O_2CR)_6(py)_3]X$ complexes (L = pyridine and substituted py, R = alkyl or aryl group, X = ClO_4^- or NO_3^-) have been synthesized and their electrochemistry in non-aqueous media examined.

Experimental

Materials

The compounds $Fe(ClO_4)_3 \cdot 6H_2O$, $Fe(NO_3)_3 \cdot 9H_2O$, acetic acid, pivalic acid, benzoic acid, 4-nitrobenzoic acid, chloroacetic acid, trichloroacetic acid, cyanoacetic acid, pyridine (py), 3-aminopyridine (3-H_2Npy), 4-aminopyridine (4-H_2Npy), 3-cyanopyridine (3-NCpy), 4-cyanopyridine (4-NCpy) and 4-vinylpyridine (4-CH_2CHpy) were obtained from commercial sources and used as received. Solvents were of standard laboratory grade unless stated otherwise. The complex $[Fe_3O(O_2CMe)_6(H_2O)_3]ClO_4 \cdot 2H_2O$ was prepared by the method of Brown *et al.*[9]

Synthesis

CAUTION: perchlorate salts of metal complexes are potentially explosive. The various $[Fe_3O(O_2CMe)_6L_3]X$ (X = ClO_4^- or NO_3^-, L = py, 3-H_2Npy, 4-H_2Npy, 3-NCpy, 4-NCpy or 4-CH_2CHpy) compounds were synthesized using a procedure

similar to that used to prepare $[Fe_3O(O_2CMe)_6(4\text{-}Etpy)_3]ClO_4$.[10] All of the compounds except $[Fe_3O(O_2CMe)_6(py)_3]ClO_4$ are described here for the first time. The method used here involved adding an excess of the free pyridine to an ethanol or acetone solution of $[Fe_3O(O_2CMe)_6(H_2O)_3]ClO_4\cdot 2H_2O$. For those ligands which are liquids the complex : ligand ratio was 1 : 100, whilst for those which are solids the ratio was 1 : 20. The products generally precipitated from solution, were collected by filtration and washed with diethyl ether before being dried in a desiccator over silica gel. Where solubility permitted, the complexes were purified by recrystallisation from dichloromethane containing a small quantity of the free pyridine. A co-solvent (*n*-pentane, diethyl ether or ethyl acetate) was generally added to induce precipitation. The $[Fe_3O(O_2CR)_6(py)_3]X$ compounds were prepared from the corresponding triaqua complexes, $[Fe_3O(O_2CR)_6(H_2O)_3]X\cdot nH_2O$, by a similar procedure. The syntheses of the latter involved the addition of hydrated $Fe(ClO_4)_3$ or $Fe(NO_3)_3$ to neutralised solutions of the appropriate carboxylic acid.[11,12] Replacement of H_2O was achieved by adding an excess of py to an ethanol solution of the corresponding triaqua complex. The compounds for which $R = CH_2CN$ or $4\text{-}NO_2C_6H_4$ and L = py are described here for the first time. Representative syntheses of $[Fe_3O(O_2CCH_2CN)_6(H_2O)_3]ClO_4\cdot 6H_2O$ and $[Fe_3O(O_2CCH_2CN)_6(py)_3]ClO_4$ are described below in detail, the analytical and spectroscopic data for the $[Fe_3O(O_2CR)_6L_3]X$ complexes being summarised in Table 1.

$[Fe_3O(O_2CCH_2CN)_6(H_2O)_3]ClO_4\cdot 6H_2O$. A solution of $NCCH_2CO_2H$ (4.07 g, 0.048 mol) in distilled water (45 cm^3) was neutralised with solid $NaHCO_3$ (4.11 g, 0.049 mol) (note vigorous effervescence of CO_2) and the resulting mixture warmed with stirring for 1 h. To this solution was added $Fe(ClO_4)_3\cdot 6H_2O$ (11.06 g, 0.024 mol) in distilled water (20 cm^3) (dropwise), forming a deep red solution. After cooling the mixture to room temperature and stirring for 3 h a microcrystalline dark red precipitate was collected by filtration, washed with diethyl ether, and dried in air (4.57 g, 68%) (Found: C, 22.5; H, 3.0; N, 8.6. Calc. for $C_{18}H_{30}ClFe_3N_6O_{26}$: C, 22.8; H, 3.2; N, 8.9%). $\tilde{\nu}_{max}/cm^{-1}$ (KBr) 3390s, 2977m, 2933m, 2274m, 1643s, 1431s, 1381s, 1298m, 1281m, 1099s, 957m, 715m, 627m, 586m, 548m and 466m.

$[Fe_3O(O_2CCH_2CN)_6(py)_3]ClO_4$. The complex $[Fe_3O(O_2CCH_2CN)_6(H_2O)_3]ClO_4\cdot 6H_2O$ (1.25 g, 1.32 mmol) was dissolved with warming (≈40–50 °C) in absolute ethanol (40 cm^3) and pyridine (11 cm^3, 0.136 mol) added dropwise, which led to the immediate formation of a fine light green precipitate. The mixture was cooled to room temperature and, after being stirred for 3 h, the product was collected by filtration, washed extensively with ethanol and diethyl ether, and dried (1.21 g, 90%).

Physical measurements

Elemental analyses (C, H, N) were performed by Microanalytical Services at University College London or Otago University. Infrared (IR) spectra were recorded using a Nicolet 210 FTIR spectrometer, positive-ion fast atom bombardment (FAB) mass spectra by the Mass Spectrometry Service UCL, with a VG ZAB 2SE mass spectrometer in 3-nitrobenzyl alcohol matrix. Electrochemical studies were carried out as described previously.[14] Voltammetric measurements were made using a three-electrode arrangement, consisting of a platinum-bead working electrode, platinum-wire auxiliary electrode and a Ag–AgCl reference electrode, against which ferrocene is oxidised at +0.55 V. The UV/VIS/NIR spectra of the mixed-valence complexes $[Fe_3O(O_2CMe)_6L_3]$ and $[Fe_3O(O_2CR)_6(py)_3]$ were collected by electrogeneration in an optically transparent thin layer electrolysis (OTTLE) cell, located in the sample compartment of a Perkin-Elmer Lambda 9 spectrophotometer,[15] using a Metrohm Polarecord E506 potentiostat, or alternatively using a Cary 5 spectrophotometer and a PAR 273 potentiostat.

Crystallography

Almost one third of a sphere of room-temperature four-circle single-counter diffractometer data was measured ($2\theta_{max} = 60°$; 2θ–θ scan mode; graphite-monochromated Mo-Kα radiation, $\lambda = 0.7107_3$ Å; $T \approx 295$ K), yielding 11 530 reflections, these being 'merged' after gaussian absorption correction to yield 2964 unique reflections ($R_{int} = 0.025$), 1918 of these with $I > 2\sigma(I)$ being considered 'observed' and used in the full-matrix least-squares refinement. Anisotropic thermal parameters were refined for the non-hydrogen atoms, $(x, y, z, U_{iso})_H$ being constrained at estimated values. Conventional residuals R, R' [statistical weights, derivative of $\sigma^2(I) = \sigma^2(I_{diff}) + 0.0004\sigma^4(I_{diff})$] were 0.043, 0.058 at convergence. As modelled in space group $P6_3/m$, the nitrate anion, lying with N on a site of $\bar{3}$ symmetry, is disordered; it was refined as a rigid body, oxygen thermal parameters isotropic. The solvent was modelled as dichloromethane, disordered about a 3 axis, chlorine site occupancy 2/3. Neutral atom complex scattering factors were employed; computation used the XTAL 3.4 program system.[16]

Crystal data. $C_{57}H_{45}Fe_3N_4O_{16}\cdot CH_2Cl_2$, $M = 1294.5$, hexagonal, space group $P6_3/m$ (C_{6h}^2, no. 176), $a = 13.345(3)$, $c = 19.24(1)$ Å, $U = 2969$ Å^3, D_c ($Z = 2$ trimers) $= 1.44_9$ g cm^{-3}, $F(000) = 1326$, $\mu_{Mo} = 8.8$ cm^{-1}, specimen $0.20 \times 0.20 \times 0.57$ mm, $A^*_{min,max} = 1.16, 1.99$.

CCDC reference number 186/933.

See http://www.rsc.org/suppdata/dt/1998/1845/ for crystallographic files in .cif format.

Results and Discussion

Synthesis and characterisation of complexes

The triaqua complex $[Fe_3O(O_2CMe)_6(H_2O)_3]ClO_4\cdot 2H_2O$[9] proved to be a convenient precursor for the preparation of a range of substituted pyridine (L) complexes of general formula $[Fe_3O(O_2CMe)_6L_3]ClO_4$, several of which are reported here for the first time. The synthesis involved the addition of an excess of the free pyridine to ethanol or acetone solutions of $[Fe_3O(O_2CMe)_6(H_2O)_3]^+$. In each case substitution of H_2O by the incoming pyridine ligand appeared to be complete, *i.e.* there was no evidence for partial substitution. The complexes, which range from yellow-green to orange-brown, were characterised by elemental analysis, IR, FAB mass spectra (Table 1) and, in the case of $[Fe_3O(O_2CPh)_6(py)_3]NO_3$, by X-ray crystallography (Table 2).

The IR spectra in general show features attributable to each component of the structure, *i.e.* the bridging acetate ligand,[17] the neutral pyridine ligand,[18] the $\{Fe_3(\mu\text{-}O)\}^{7+}$ core[19] and the counter ion.[20] Bands from the asymmetric and symmetric stretching $\nu(CO_2)$ modes of acetate are found in the region ≈1595 and ≈1450 cm^{-1} respectively, consistent with a bridging co-ordination mode.[17] Internal ligand bands from the pyridine bases are also observed; the potentially ambidentate 3-NCpy and 4-NCpy ligands co-ordinate *via* the heterocyclic N atom, as shown by IR spectroscopy; $\nu(CN)$ was found at 2241 and 2242 cm^{-1}, *cf.* 2232 and 2244 cm^{-1} for free 3-NCpy and 4-NCpy respectively. In cases where 3(or 4)-NCpy co-ordinates *via* the cyano N larger shifts in $\nu(CN)$ are typically observed.[21,22]

Positive-ion FAB mass spectra show retention of the $[Fe_3O(O_2CMe)_6]^+$ core ($m/z = 538$) and incorporation of L, *e.g.* for $[Fe_3O(O_2CMe)_6(py)_3]^+$ peaks are observed at $m/z = 696$ and 617, corresponding to $[Fe_3O(O_2CMe)_6(py)_2]^+$ and $[Fe_3O(O_2CMe)_6(py)]^+$ respectively (Table 1). Fragments of the core are also observed at $m/z = 479$ $\{[Fe_3O(O_2CMe)_5]^+\}$, 420 $\{[Fe_3O(O_2CMe)_4]^+\}$ and 361 $\{[Fe_3O(O_2CMe)_3]^+\}$ for all of the acetate complexes. In some cases the matrix was found to incorporate

Table 1 Summary of analytical and spectroscopic data for $[Fe_3O(O_2CR)_6L_3]X$ complexes

$[Fe_3O(O_2CR)_6(L)_3]X$				Analysis[b] (%)				
R	L	Yield[a] (%)	Colour	C	H	N	IR[c]/cm^{-1}	FAB mass spectrum[d]/*m*/*z* (% base peak)
Me	py[e,f]	61	Yellow-green	36.6 (37.08)	3.6 (3.80)	4.7 (4.81)	1595, 1448[g]	696 (11, $M^+ - L$), 617 (49, $M^+ - 2L$)[h]
Me	3-H_2Npy[e,i]	26	Light brown	35.2 (35.26)	3.9 (3.95)	9.2 (9.14)	1586, 1448, ν_{NH} 3472, 3374	*j*
Me	4-H_2Npy[e,i,k]	55	Yellow-green	32.5 (32.70)	4.1 (4.47)	7.9 (8.48)	1590, 1444 ν_{NH} 3472, 3374	726 (11, $M^+ - L$), 665 (12, $M^+ - O_2CR$), 632 (33, $M^+ - 2L$), 573 (15, $M^+ - 2L - O_2CR$)[h]
Me	3-NCpy[e,i,l]	76	Brown-apricot	36.3 (37.94)	3.1 (3.19)	8.2 (8.85)	1594, 1450 ν_{CN} 2241	642 (13, $M^+ - 2L$)[h]
Me	4-NCpy[e,f,l]	26	Brown	36.9 (37.94)	3.1 (3.19)	9.0 (8.85)	1595, 1448 ν_{CN} 2242	642 (3, $M^+ - 2L$)[h]
Me	4-CH_2CHpy[e,f]	76	Green	41.4 (41.60)	3.9 (4.13)	4.4 (4.37)	1598, 1439	624 (24, $M^+ - 2L$)[h]
Bu^t	py[e,i]	36	Green	47.4 (47.95)	6.0 (6.17)	3.5 (3.73)	1588, 1427[g]	1027 (2, M^+), 948 (12, $M^+ - L$), 869 (32, $M^+ - 2L$), 790 (100, $M^+ - 3L$)
Ph	py[f,l,m,n]	68	Brown	52.4 (53.81)	3.5 (3.66)	4.2 (4.33)	1604, 1566, 1410, 1350[g,o]	1068 (6, $M^+ - L$), 989 (24, $M^+ - 2L$), 910 (100, $M^+ - 3L$)
CH_2Cl	py[e,f,p]	80	Green	32.3 (31.61)	2.6 (2.65)	4.3 (4.38)	1624, 1430[g]	823 (22, $M^+ - 2L$), 743 (33, $M^+ - 3L$), 710 (40, $M^+ - 3L - Cl$), 651 (23, $M^+ - 3L - O_2CR$), 558 (27, $M^+ - 3L - 2O_2CR$), 463 (20, $M^+ - 3L - 3O_2CR$)
CCl_3	py[e,i,q]	74	Orange-brown	26.2 (26.69)	1.3 (1.52)	4.0 (4.23)	1650, 1382[g]	*r*
CH_2CN	py[e,f]	80	Light-green	38.1 (38.68)	2.3 (2.61)	12.0 (12.31)	1640, 1428[g] ν_{CN} 2263	*j*
$C_6H_4NO_2$-4[s]	py[e,f]	66	Yellow-green	45.1 (45.13)	3.0 (2.59)	7.9 (8.31)	1625, 1589, 1419, 1347, ν_{NO_2} 1527, 1320[g,o]	1259 (23, $M^+ - 2L$), 1180 (57, $M^+ - 3L$), 1014 (74, $M^+ - 3L - O_2CR$), 848 (90, $M^+ - 3L - 2O_2CR$), 682 (100, $M^+ - 3L - 3O_2CR$)

[a] Yield based on $[Fe_3O(O_2CR)_6(H_2O)_3]X\cdot nH_2O$. [b] Calculated values in parentheses. [c] Recorded as KBr discs. The first two bands listed correspond to the asymmetric and symmetric ν_{CO_2} bands respectively, except in the case of R = Ph and $C_6H_4NO_2$-4 (see *o*). The IR spectra of ClO_4^- salts reveal a strong, structured band at ≈1100 cm^{-1} (ν_3) and, in some cases, a weaker band at ≈625 cm^{-1} (ν_4) is also observed when not masked by other ligand vibrations. For NO_3^- salts, ν_3 typically occurs at ≈1385 cm^{-1}. [d] Recorded in 3-nitrobenzyl alcohol matrix, *m*/*z* = 153. [e] X = ClO_4^-. [f] Absolute ethanol reaction solvent. [g] Complexes where L = py display bands at *ca.* 1492 (19a), 1449 (19b), 1221 (9a), 1034 (12), 1015 (1), 761–754 (4), 702–689 (11), 623 (6a or 6b) and 428 cm^{-1} (16b) due to internal ring modes classified using the notation described in ref. 13. The mode number is given in parentheses after the band location. [h] All acetate-bridged complexes display peaks at *m*/*z* = 538 ($M^+ - 3L$), 479 ($M^+ - 3L - O_2CMe$), 420 ($M^+ - 3L - 2O_2CMe$) and 361 ($M^+ - 3L - 3O_2CMe$). [i] Acetone reaction solvent. [j] Low solubility in matrix. [k] Calculated for $[Fe_3O(O_2CMe)_6(4\text{-}H_2Npy)_3]ClO_4\cdot 4H_2O$. [l] Repeatedly gave low carbon analysis. [m] X = NO_3^-. [n] Calculated for $[Fe_3O(O_2CPh)_6(py)_3]NO_3\cdot CH_2Cl_2$. [o] The ν_{CO_2} region of aromatic carboxylates is complicated by in-plane C–C ring and C–H deformations from the aryl group. For the present complexes, R = Ph and $C_6H_4NO_2$-4, several bands are observed in the 1700–1400 cm^{-1} region, and definite assignments could not be made. [p] Calculated for $[Fe_3O(O_2CCH_2Cl)_6(py)_3]ClO_4\cdot 0.5py$. [q] Calculated for $[Fe_3O(O_2CCCl_3)_6(py)_3]ClO_4\cdot 2py$. [r] Decomposed in dichloromethane. [s] The nitro group is located in the 4 position of the aromatic ring.

into the ion, giving rise to peaks at *m*/*z* = 691, 631 and 572, these corresponding to $[Fe_3O(O_2CMe)_6(O_2NC_6H_4CH_2OH)]^+$, $[Fe_3O(O_2CMe)_5(O_2NC_6H_4CH_2OH)]^+$ and $[Fe_3O(O_2CMe)_4(O_2NC_6H_4CH_2OH)]^+$ respectively. Previous mass spectral studies have led to the detection of species with larger aggregates,[23–25] but this was not the case here.

The $[Fe_3O(O_2CR)_6(py)_3]X$ compounds were prepared by adding an excess of pyridine to ethanol solutions of the corresponding triaqua complexes, $[Fe_3O(O_2CR)_6(H_2O)_3]X\cdot nH_2O$, the latter having been isolated from aqueous solutions of Fe^{3+} and ^-O_2CR. Analytical and spectroscopic data for these complexes are listed in Table 1. The $\nu(CO_2)$ region of the IR spectra are dependent upon the identity of R,[26] and also contain bands due to the internal modes of co-ordinated py.[13,27,28] The FAB mass spectra are in general similar to those of the acetate complexes, *e.g.* for R = Bu^t the molecular ion was observed at *m*/*z* = 1027 $\{[Fe_3O(O_2CBu^t)_6(py)_3]^+\}$, as were fragments due to the loss of py ligands at *m*/*z* = 948, 869 and 790 for $[Fe_3O(O_2CBu^t)_6(py)_2]^+$, $[Fe_3O(O_2CBu^t)_6(py)]^+$ and $[Fe_3O(O_2CBu^t)_6]^+$ respectively, and loss of carboxylates at *m*/*z* = 689, 588 and 386 corresponding to $[Fe_3O(O_2Bu^t)_5]^+$, $[Fe_3O(O_2CBu^t)_4]^+$ and $[Fe_3O(O_2CBu^t)_3]^+$ respectively. Satisfactory spectra could not be obtained for some of the less soluble complexes.

Dark orange-red hexagonal crystals of $[Fe_3O(O_2CPh)_6(py)_3]NO_3$ were obtained upon slow evaporation of a dichloromethane–ethyl acetate solution (1:1). The results of the room-temperature single crystal X-ray study are consistent with formulation of the complex, in terms of stoichiometry and connectivity, as $[Fe_3O(O_2CPh)_6(py)_3]NO_3\cdot CH_2Cl_2$, the cation being depicted in Fig. 1, with selected bond lengths and angles given in Table 2. The structure is of high symmetry; however, the anion and solvent molecules are modelled as disordered, the latter lying with their carbon atoms disposed on a crystallographic 3 axis, as modelled in the space group $P6_3/m$, interleaving the cations which lie with their central oxygen atoms disposed on sites of $\bar{6}$ crystallographic symmetry, with implicit mirror planes normal to the 3 axis passing through the $OFe_3(py)_3$ component, and relating the two halves of the py molecules, and pairs of carboxylate ligands. The three iron atoms form an obligate equilateral triangle, the oxygen atom lying at its centre with the pyridine ring planes perpendicular to it and the benzoate C_7O_2 plane inclined to it with a dihedral angle of 42.06(4)°. The co-ordination environment about each iron atom is approximately octahedral, each iron atom being displaced by 0.192 Å towards the central bridging oxygen atom from the plane defined by the four benzoate oxygen atoms. The Fe–O (central) (1.908 Å) and the Fe–N (*trans* thereto, 2.196 Å) are the shortest and longest bond distances respectively in the

Table 2 Selected bond lengths (Å) and angles (°) for $[Fe_3O(O_2CPh)_6(py)_3]NO_3{\cdot}CH_2Cl_2$ (estimated standard deviations in parentheses)

Fe–O(0)	1.9084(5)	C(1)–C(11)	1.495(4)
Fe–O(11)	2.011(2)	C(11)–O(11)	1.256(3)
Fe–N(11)	2.196(2)	C(11)–O(12)	1.258(2)
Fe–O(12^{I})	2.003(3)	Fe ··· Fe	3.306(1)
O(0)–Fe–O(11)	95.23(5)	C(11)–C(1)–C(6)	119.9(2)
O(0)–Fe–N(11)	179.08(9)	C(2)–C(1)–C(6)	119.9(3)
O(0)–Fe–O(12^{I})	95.76(5)	C(1)–C(11)–O(11)	117.4(2)
O(11)–Fe–N(11)	84.12(8)	C(1)–C(11)–O(12)	117.7(2)
O(11)–Fe–O(12^{I})	89.2(1)	O(11)–C(11)–O(12)	124.9(3)
O(11)–Fe–O(11^{II})	90.2(1)	Fe–O(11)–C(11)	132.9(2)
O(11)–Fe–O(12^{III})	169.01(6)	C(11)–O(12)–Fe^{IV}	132.8(2)
N(11)–Fe–O(12^{I})	84.89(9)	Fe–N(11)–C(12)	120.5(1)
O(12^{I})–Fe–O(12^{III})	89.3(1)	C(12)–N(11)–C(12^{II})	119.0(2)
C(11)–C(1)–C(2)	120.2(2)		

Transformations of the asymmetric unit: I $y-x, 1-x, z$; II $x, y, \frac{3}{2}-z$; III $y-z, 1-z, \frac{3}{2}-z$; IV $1-y, 1+x-y, z$.

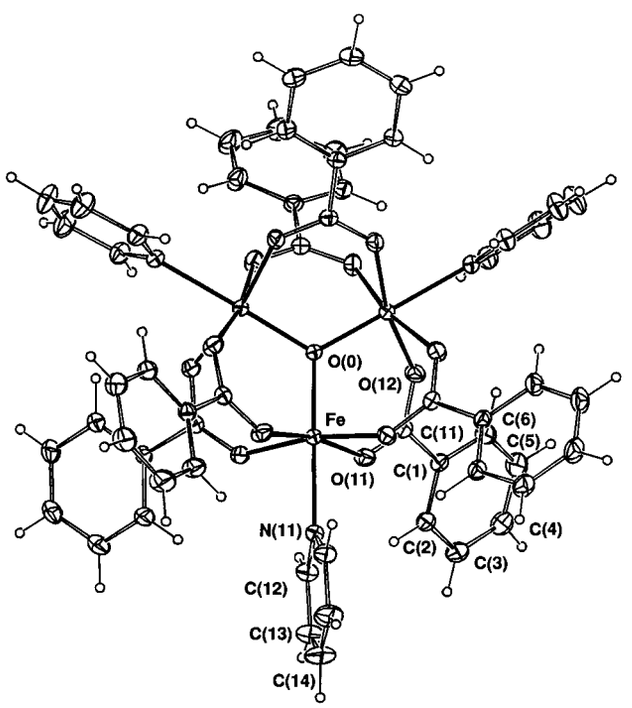

Fig. 1 Projection of the $[Fe_3O(O_2CPh)_6(py)_3]^+$ cation; 20% thermal ellipsoids are shown for the non-hydrogen atoms, hydrogen atoms having arbitrary radii of 0.1 Å

$FeNO_5$ environment, Fe–O (benzoate) (2.003–2.011 Å) being intermediate. The FeO_5 geometry is similar to that found in related structures.[29,30]

Redox behaviour of $[Fe_3O(O_2CR)_6L_3]^+$ complexes

General redox behaviour. The redox properties of the various $[Fe_3O(O_2CMe)_6L_3]ClO_4$ and $[Fe_3O(O_2CR)_6(py)_3]X$ complexes were initially examined by cyclic voltammetry in 0.2 mol dm^{-3} $[NBu_4][PF_6]$–dichloromethane, in the presence and absence of free py or substituted py and the results are summarised in Tables 3 and 4. In the presence of an excess of a free pyridine, these complexes in general display a chemically reversible reduction in the region +0.5 to −0.2 V (*vs.* Ag–AgCl), attributed to the one-electron reduction of the monocationic $[Fe_3O(O_2CR)_6L_3]^+$ complex to the neutral mixed-valence form $[Fe_3O(O_2CR)_6L_3]$ [equation (1)]. For the acetate-bridged com-

$$[Fe_3O(O_2CR)_6L_3]^+ \overset{+e^-}{\rightleftharpoons} [Fe_3O(O_2CR)_6L_3]^0 \qquad (1)$$

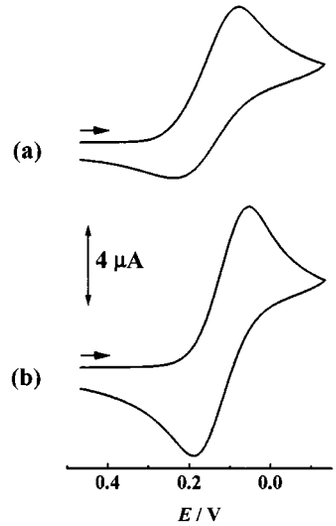

Fig. 2 Room-temperature cyclic voltammetry of $[Fe_3O(O_2CMe)_6(3\text{-}NCpy)_3]ClO_4$ in 0.2 mol dm^{-3} $[NBu_4][PF_6]$–dichloromethane (a), and after the addition of free 3-NCpy (b). Scan rate = 100 mV s^{-1}

plexes, $[Fe_3O(O_2CMe)_6L_3]^+$, the reduction is partially reversible ($I_{pa}/I_{pc} < 1.0$)[31a] or in some cases even irreversible in the absence of L (Table 3).[32] The cyclic voltammograms of $[Fe_3O(O_2CMe)_6(3\text{-}NCpy)_3]^+$ prior to, and after, the addition of free 3-NCpy are shown in Fig. 2. Upon the addition of 3-NCpy to the electrochemical solution the cathodic response becomes typical of that for a chemically reversible one-electron process, *i.e.* $I_{pa}/I_{pc} \approx 1.0$, $\Delta E_p = 110$ mV (at 100 mV s^{-1}), where ΔE_p increases with increasing scan rate over the range 100–1000 mV s^{-1} (electrochemically quasi-reversible). The ΔE_p for ferrocene–ferrocenium is 60–65 mV under identical experimental conditions, and is unchanged with increasing scan-rate. The fact that the first reduction process is irreversible in the absence of free pyridine, and reversible in the presence of free pyridine, suggests that the cause of irreversibility is associated with the loss of ligand from the neutral $[Fe_3O(O_2CMe)_6(3\text{-}NCpy)_3]$ species [equation (2)]. A second irreversible reduction can also be

$$[Fe_3O(O_2CR)_6L_3]^+ \overset{+e^-}{\rightleftharpoons} [Fe_3O(O_2CR)_6L_3]^0 \longrightarrow [Fe_3O(O_2CR)_6L_2]^0 + L \qquad (2)$$

observed at considerably more negative potentials (*ca.* −0.9 V), however this process is irreversible under all conditions examined. For the $[Fe_3O(O_2CR)_6(py)_3]^+$ complexes (Table 4) the first reduction is generally chemically reversible ($I_{pa}/I_{pc} \approx 1.0$) both in the presence and absence of free py. The second reduction is again chemically irreversible in the absence of free pyridine and remains so following the addition of py for all but one of the complexes. The notable exception is the cyanoacetate-bridged species, $[Fe_3O(O_2CCH_2CN)_6(py)_3]^+$, the results for which are described below in more detail.

Further reduction of $[Fe_3O(O_2CR)_6(py)_3]$. Complexes $[M_3O(O_2CR)_6(py)_3]^z$ of second- and third-row transition metals tend to display a number of reversible, one-electron processes.[3e,33] By contrast, those $[M_3O(O_2CR)_6(py)_3]^z$ complexes of first-row transition metals have at best exhibited only one reversible electron-transfer step.[3f,8f,h,i] The complexes described herein behave similarly, with the exception of $[Fe_3O(O_2CCH_2CN)_6(py)_3]ClO_4$ which, in the presence free pyridine, displays a second, reversible reduction. The cyclic voltammogram of $[Fe_3O(O_2CCH_2CN)_6(py)_3]ClO_4$ in $[NBu_4][PF_6]$–dichloromethane is shown in Fig. 3. The reversible $[Fe_3O(O_2CCH_2CN)_6(py)_3]^{+/0}$ reduction is found at a moderately positive potential, $E_{\frac{1}{2}} = +0.46$ V [Fig. 3(a)]. Scanning to more cathodic potentials reveals the irreversible second reduction

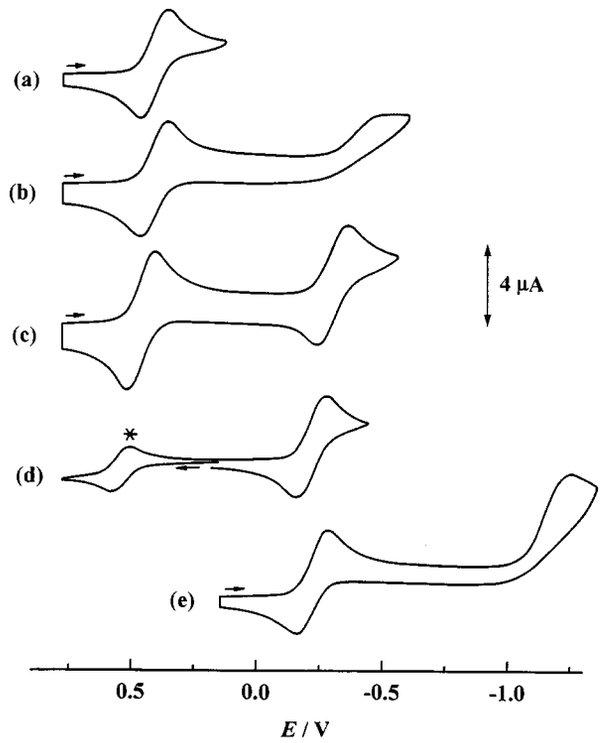

Fig. 3 (a), (b) Cyclic voltammetry of $[Fe_3O(O_2CCH_2CN)_6(py)_3]ClO_4$ in 0.2 mol dm^{-3} $[NBu_4][PF_6]$–dichloromethane at room temperature, (c) in the presence of py. (d), (e) Cyclic voltammetry of $[Fe_3O(O_2CBu^t)_6(py)_3]ClO_4$ in 0.2 mol dm^{-3} $[NBu_4][PF_6]$–dichloromethane–py. In each case the scan rate = 100 mV s^{-1}. The asterisk in (d) marks the oxidation of internal ferrocene, +0.55 V

with $E_{pc} \approx -0.5$ V [Fig. 3(b)]. Notably, the height of the return wave associated with the $[Fe_3O(O_2CCH_2CN)_6(py)_3]^{+/0}$ reduction remains unaffected after scanning over this second reduction. Upon the addition of free py to the electrochemical solution the appearance of the second reduction process changes markedly [Fig. 3(c)]. The forward wave becomes well defined and a return wave is clearly observed on the reverse scan ($I_{pa}/I_{pc} \approx 0.9$, $E_{\frac{1}{2}} = -0.27$ V). Rotating-disc voltammetry indicates that both of the reductive processes involve the same number of electrons, such that the second reduction represents the formation of the previously undetected monoanionic complex $[Fe_3O(O_2CCH_2CN)_6(py)_3]^-$, a further mixed-valence species which formally contains a single Fe^{III} and two Fe^{II}. The reversibility of the $[Fe_3O(O_2CCH_2CN)_6(py)_3]^{0/-}$ reduction implies that the monoanion has a well defined lifetime, being stable on the timescale of the voltammetric experiment. The redox changes displayed by the $[Fe_3O(O_2CCH_2CN)_6(py)_3]^+$ ion are summarised in equation (3). The redox behaviour of $[Fe_3O(O_2CCH_2CN)_6(py)_3]ClO_4$ can be contrasted with that of other related complexes such as the pivalate-bridged complex $[Fe_3O(O_2CBu^t)_6(py)_3]ClO_4$ [Fig. 3(d), (e)]. Under identical experimental conditions this complex displays a reversible reduction with $E_{\frac{1}{2}} = -0.21$ V $\{[Fe_3O(O_2CBu^t)_6(py)_3]^{+/0}\}$, and a second reduction which remains irreversible even in the presence of free py.

$$[Fe_3O(O_2CCH_2CN)_6(py)_3]^+ \overset{+e^-}{\rightleftharpoons} [Fe_3O(O_2CCH_2CN)_6(py)_3]^0$$
$$Fe^{III}Fe^{III}Fe^{III} \qquad Fe^{III}Fe^{III}Fe^{II}$$
$$\overset{+e^-}{\rightleftharpoons} [Fe_3O(O_2CCH_2CN)_6(py)_3]^- \quad (3)$$
$$Fe^{III}Fe^{II}Fe^{II}$$

Dependence of $E_{\frac{1}{2}}$ of $[Fe_3O(O_2CMe)_6L_3]^{+/0}$ and $[Fe_3O(O_2CR)_6(py)_3]^{+/0}$ on L and R. The reversible $E_{\frac{1}{2}}$ potentials for the $[Fe_3O(O_2CMe)_6L_3]^{+/0}$ reductions are quite sensitive both to the identity and the location of substituent on the pyridine ring, *i.e.* for the same substituent at the 3 and 4 positions of the pyridine ring $E_{\frac{1}{2}}$ varies by as much as 0.12 V (for 3-H_2Npy *vs.* 4-H_2Npy). Similarly $E_{\frac{1}{2}}$ for $[Fe_3O(O_2CR)_6(py)_3]^{+/0}$ is strongly dependent on the identity of the bridging carboxylate ligand, varying from +0.46 V for $^-O_2CCH_2CN$ to −0.21 V for $^-O_2CBu^t$. These variations in reduction potential can be rationalised by comparing the inductive influence of the different groups; as expected, electron-withdrawing groups move the reduction potential to more positive potentials, whilst electron-donating groups have the opposite effect. The magnitude of the effect can be related to the pK_a of the respective ligands,[34,35] with $E_{\frac{1}{2}}$ for $[Fe_3O(O_2CMe)_6L_3]^{+/0}$ and $[Fe_3O(O_2CR)_6(py)_3]^{+/0}$ varying linearly with the pK_a of L and ^-O_2CR respectively (Fig. 4). Linear regression analysis of the plots of $E_{\frac{1}{2}}$ *vs.* pK_a for L or ^-O_2CR give equations (4) and (5) respectively. The influence of the

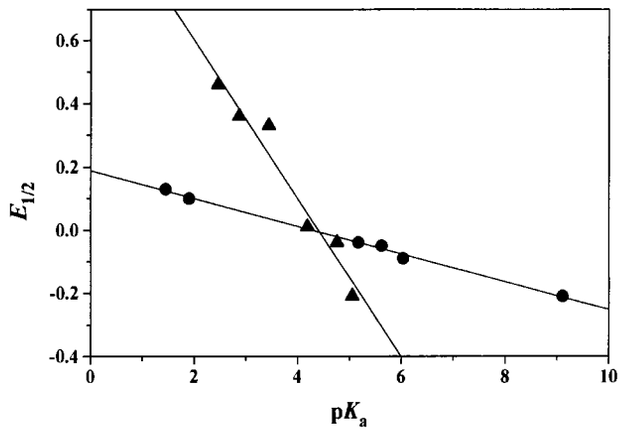

Fig. 4 Plots of potential $E_{\frac{1}{2}}$ *vs.* ligand pK_a values for $[Fe_3O(O_2CMe)_6L_3]ClO_4$ (●) and $[Fe_3O(O_2CR)_6(py)_3]ClO_4$ (▲). Lines of best fit, calculated by linear regression analysis, are shown

$$E_{\frac{1}{2}} = 0.188 - 0.044(pK_a) \quad R = 0.99 \qquad (4)$$

$$E_{\frac{1}{2}} = 1.105 - 0.251(pK_a) \quad R = 0.98 \qquad (5)$$

carboxylate substituent is clearly more important in determining the potential of the reduction, with the gradient of $E_{\frac{1}{2}}$ *vs.* pK_a for ^-O_2CR being nearly six times that for Rpy. A recent study of three $[Fe_3O(O_2CR)_6(py)_3]^+$ complexes (R = Me, Ph or CCl_3) in neat pyridine found a good correlation between $E_{\frac{1}{2}}$ for $[Fe_3O(O_2CR)_6(py)_3]^{+/0}$ and the Hammett parameter, σ_p,[8h] whilst for $[Ru_3O(O_2CMe)_6L_3]$ ions (where L = substituted pyridine or pyrazine) $E_{\frac{1}{2}}$ varied linearly with pK_a of L,[33b] as was found in this work.

Ligand-based processes. Only in the case of $[Fe_3O(O_2CMe)_6(3\text{-}H_2Npy)_3]^+$ and $[Fe_3O(O_2CMe)_6(4\text{-}H_2Npy)_3]^+$ oxidative processes were detected. For these complexes broad irreversible waves were observed at $E_{pa} \approx +1.3$ V for both $[Fe_3O(O_2CMe)_6(3\text{-}H_2Npy)_3]^+$ and $[Fe_3O(O_2CMe)_6(4\text{-}H_2Npy)_3]^+$. Repeated scanning over these waves resulted in a gradual decrease in the peak current, and eventually led to passivation of the electrode. This irreversible process can be attributed to the oxidation of H_2Npy ligands.

Spectroelectrochemical studies

In situ electrochemical reduction of the $[Fe_3O(O_2CMe)_6L_3]^+$ and $[Fe_3O(O_2CR)_6(py)_3]^+$ complexes at room temperature in an OTTLE cell enabled the chemical reversibility of the $[Fe_3O(O_2CR)_6L_3]^{+/0}$ couple to be determined on the spectroelectrochemical timescale and, in cases where the reduction was found to be chemically reversible, permitted characterisation of the neutral mixed-valence species by electronic absorption spectroscopy (Table 5). Several of the complexes could not be

Table 3 Cyclic voltammetric data for $[Fe_3O(O_2CMe)_6L_3]ClO_4$ complexes

Complex	$E_{\frac{1}{2}}^{a}$/V	ΔE_p^{b}/mV	$I_{pa}/I_{pc}^{b,c}$
$[Fe_3O(O_2CMe)_6(py)_3]ClO_4$	−0.04	110 (q-rev)	1.1 (0.7)
$[Fe_3O(O_2CMe)_6(3\text{-}H_2Npy)_3]ClO_4$	−0.09	80 (rev)	1.0 (0.7)
$[Fe_3O(O_2CMe)_6(4\text{-}H_2Npy)_3]ClO_4$	−0.21	70 (rev)	1.0 (0.9)
$[Fe_3O(O_2CMe)_6(3\text{-}NCpy)_3]ClO_4$	+0.13	110 (q-rev)	1.0 (0.7)
$[Fe_3O(O_2CMe)_6(4\text{-}NCpy)_3]ClO_4$	+0.10	80 (rev)	1.1 (0.7)
$[Fe_3O(O_2CMe)_6(4\text{-}CH_2CHpy)_3]ClO_4$	−0.05	95 (rev)	1.0 (0.8)

[a] Dichloromethane solutions for voltammetric measurements were 0.2 mol dm^{-3} in $[NBu_4][PF_6]$ and $\approx 1 \times 10^{-3}$ mol dm^{-3} in complex. Free L, $\approx 10 \times 10^{-3}$ mol dm^{-3}, was added to the electrochemical solution after dissolving the complex. All tabulated values were recorded at room temperature. Potentials are quoted *vs.* the Ag–AgCl reference electrode, against which ferrocene–ferrocenium occurs at +0.55 V. rev = Reversible, q-rev = quasi-reversible (as determined by CV,[31a] where a reversible process is defined as one where $I_{pa}/I_{pc} = 1.0$ and ΔE_p is constant with increasing scan rate, whereas for a quasi-reversible process $I_{pa}/I_{pc} = 1.0$ and ΔE_p increases with increasing scan rate); $E_{\frac{1}{2}} = (E_{pa} + E_{pc})/2$. In each case a less well defined, irreversible second reduction was located at more negative potentials, in the region −0.9 to −1.0 V. [b] $\Delta E_p = E_{pc} - E_{pa}$, scan rate = 100 mV s^{-1}. [c] I_{pa}/I_{pc} ratio determined by the method given in ref. 31(*b*). Value in parentheses refers to the I_{pa}/I_{pc} ratio in the absence of free L.

Table 4 Cyclic voltammetric data for $[Fe_3O(O_2CR)_6(py)_3]X$ complexes

	First reduction, $[Fe_3O(O_2CR)_6(py)_3]^{+/0}$			Second reduction
Complex[a]	$E_{\frac{1}{2}}^{b}$/V	ΔE_p^{c}/mV	I_{pa}/I_{pc}^{d}	E_{pc}^{e}/V
$[Fe_3O(O_2CBu^t)_6(py)_3]X$	−0.21	100 (q-rev)	1.0	−1.3
$[Fe_3O(O_2CMe)_6(py)_3]X$	−0.04	110 (q-rev)	1.1	−0.9
$[Fe_3O(O_2CPh)_6(py)_3]X$	+0.01	100 (q-rev)	1.0	−0.8
$[Fe_3O(O_2CC_6H_4NO_2\text{-}4)_6(py)_3]X$	+0.33	70 (q-rev)	0.9	−0.4
$[Fe_3O(O_2CCH_2Cl)_6(py)_3]X$	+0.36	95 (rev)	1.0	−0.5
$[Fe_3O(O_2CCCl_3)_6(py)_3]X$	*f*	—	—	—
$[Fe_3O(O_2CCH_2CN)_6(py)_3]X$	+0.46	80 (rev)	1.0	−0.27 [g]

[a] X = ClO_4^- for all complexes except R = Ph, where X = NO_3^-. [b] Dichloromethane solutions for voltammetric measurements were 0.2 mol dm^{-3} in $[NBu_4][PF_6]$ and $\approx 1 \times 10^{-3}$ mol dm^{-3} in complex. Free py, $\approx 10 \times 10^{-3}$ mol dm^{-3}, was added to the solution after dissolving the complex. All tabulated values were recorded at room temperature. Potentials are quoted *vs.* the Ag–AgCl reference electrode, against which ferrocene–ferrocenium occurs at +0.55 V. rev = Reversible, q-rev = quasi-reversible (as determined by CV,[31a] where a reversible process is defined as one where $I_{pa}/I_{pc} = 1.0$ and ΔE_p is constant with increasing scan rate, whereas for a quasi-reversible process $I_{pa}/I_{pc} = 1.0$ and ΔE_p increases with increasing scan rate). $E_{\frac{1}{2}} = (E_{pa} + E_{pc})/2$. [c] $\Delta E_p = E_{pc} - E_{pa}$, scan rate = 100 mV s^{-1}. [d] I_{pa}/I_{pc} ratio determined by the method given in ref. 31(*b*), scan rate = 100 mV s^{-1}. [e] The second reduction was irreversible for all complexes except R = CH_2CN. [f] Displayed only ill defined processes. Complex decomposes in dichloromethane–$[NBu_4][PF_6]$–py medium. [g] $E_{\frac{1}{2}}$ for $[Fe_3O(O_2CCH_2CN)_6(py)_3]^{0/-}$, $\Delta E_p = 100$ mV, $I_{pa}/I_{pc} = 0.9$, under the same experimental conditions as stated in *a*.

Table 5 The VIS/NIR solution spectral data (cm^{-1}) of $[Fe_3O(O_2CMe)_6L_3]^z$ and $[Fe_3O(O_2CR)_6(py)_3]^z$ complexes, $z = 1+$ and 0

		Complex	
R	L	$[Fe_3O(O_2CR)_6L_3]^+$	$[Fe_3O(O_2CR)_6L_3]$
Me	py	9400, 17 600, 21 200	9000, ≈18 000 (sh), ≈21 000 (sh), ≈24 000 (sh), 29 000
Me	4-H_2Npy	10 000, 17 100, 26 300, 31 500	*b*
Me	3-NCpy	9600, 17 900, 21 200, ≈24 400 (sh), 28 300	8500, ≈18 000 (sh), 21 000, ≈24 000, 28 600
Me	4-NCpy	9700, 18 000, 21 200, ≈24 200 (sh), 28 300	10 000, ≈18 000 (sh), 21 200, ≈24 000, 28 500
Me	4-CH_2CHpy	9300, 17 500, 21 200	*b*
Bu^t	py	9200, 17 400, 21 100, ≈24 200 (sh)	8900, ≈12 300, ≈17 500 (sh), ≈21 200 (sh), 24 000 (sh)
Ph	py	9200, 17 600, 21 200	7400, ≈17 000 (sh)
CH_2Cl	py	9000, ≈18 000 (sh), ≈21 500 (sh)	7800, ≈18 000 (sh), ≈21 000 (sh), 28 200
CH_2CN	py	9500, ≈17 000 (sh), ≈21 000 (sh)	*b*

[a] All complexes were ClO_4^- salts except for R = Ph, where X = NO_3^-. The complexes $[Fe_3O(O_2CMe)_6(3\text{-}H_2Npy)_3]ClO_4$ and $[Fe_3O(O_2CC_6H_4NO_2\text{-}4)_6(py)_3]ClO_4$ were not sufficiently soluble to collect meaningful electronic spectra, whilst $[Fe_3O(O_2CCCl_3)_6(py)_3]ClO_4$ was unstable in dichloromethane, hence these complexes are not tabulated. Electronic spectra recorded at room temperature in an OTTLE cell, in 0.2 mol dm^{-3} $[NBu_4][PF_6]$ in dichloromethane in the presence of a small excess of L ($\approx 10 \times 10^{-3}$ mol dm^{-3}). The spectra of $[Fe_3O(O_2CR)_6L_3]$ species are listed only in cases where the reduction proceeded with isosbestic points, and reoxidation led to the recovery of the starting $[Fe_3O(O_2CR)_6L_3]^+$ spectrum. sh = Shoulder. [b] Reduction was irreversible.

studied on account of the combination of their low solubility in the $[NBu_4][PF_6]$–dichloromethane medium and the low intensities of the transitions under examination.

Although the colours of the isolated $[Fe_3O(O_2CMe)_6L_3]X$ and $[Fe_3O(O_2CR)_6(py)_3]X$ complexes vary considerably, their VIS/NIR solution spectra are all quite similar [Fig. 5(a)]. The spectra contain a weak band in the region 9000–10 000 cm^{-1} ($\varepsilon \approx 10$–30 dm^3 mol^{-1} cm^{-1}) and a more intense feature near 17 000–18 000 cm^{-1} ($\varepsilon \approx 120$–150 dm^3 mol^{-1} cm^{-1}), which is sometimes present only as a shoulder on another band at higher wavenumber. The first of these bands can be assigned to an octahedral iron(III) ligand-field transition, $^6A_{1g} \longrightarrow {}^4T_{1g}$. The second band ordinarily observed in the spectra of iron(III) complexes, the $^6A_{1g} \longrightarrow {}^4T_{2g}$ transition,[36,37] should occur at higher energy but is not observed for the tris(pyridine) complexes. The $^6A_{1g} \longrightarrow {}^4T_{1g}$ and $^6A_{1g} \longrightarrow {}^4T_{2g}$ ligand-field bands have been observed in the regions 10 000–12 000 and 14 000–16 000 cm^{-1} respectively for a range of $[Fe_3O(O_2CR)_6(H_2O)_3]^+$ complexes.[38] The wavenumber of the $^6A_{1g} \longrightarrow {}^4T_{1g}$ transition is in accord with the respective positions of py and H_2O ligands in the spectrochemical series.[39] The intensities of these ligand-field bands are higher than is typically observed for high-spin octahedral iron(III) complexes.[37] The mechanism by which these transitions gain intensity is thought to be associated with the antiferromagnetic exchange interactions prevalent in these complexes.[12] There is some disagreement within the literature as to

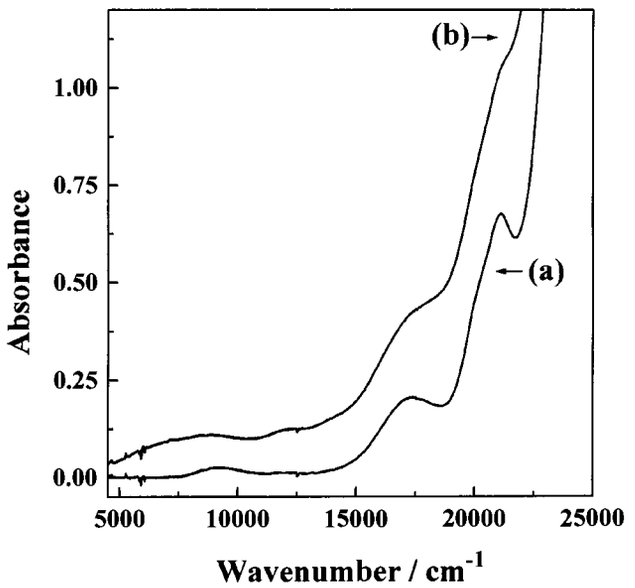

Fig. 5 The VIS/NIR spectra of (a) $[Fe_3O(O_2CBu^t)_6(py)_3]^+$ and (b) electrogenerated $[Fe_3O(O_2CBu^t)_6(py)_3]$, recorded in an OTTLE cell in 0.2 mol dm^{-3} $[NBu_4][PF_6]$–dichloromethane

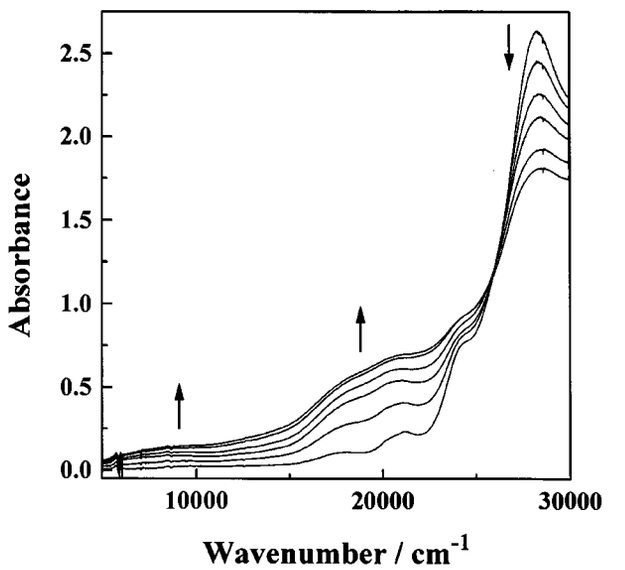

Fig. 6 The UV/VIS/NIR spectral changes accompanying reduction of $[Fe_3O(O_2CMe)_6(4\text{-}NCpy)_3]ClO_4$ in $[NBu_4][PF_6]$–dichloromethane–4-NCpy at room temperature in an OTTLE cell. Reoxidation regenerates the starting spectrum

the identity of the band in the vicinity of 17 000–18 000 cm^{-1}. It has been assigned to a simultaneous excitation of two iron(III) centres to the $^4T_{1g}(G)$ level,[7] although the energy of a 'double excitation' is anticipated to occur at twice that of the $^6A_{1g} \longrightarrow {}^4T_{1g}$ transition; however, the band is generally observed at a wavenumber ≈1000 cm^{-1} less than twice that of the $^6A_{1g} \longrightarrow {}^4T_{1g}$ transition. An alternative assignment for the band at 17 000–18 000 cm^{-1} may be to the $^6A_{1g} \longrightarrow (^4A_{1g}, {}^4E_g)$ 'spin flip'.[40] The next feature in the absorption spectrum is a relatively sharp band at *ca.* 21 000 cm^{-1} ($\varepsilon \approx 400$ dm^3 mol^{-1} cm^{-1}), with a shoulder that varies in prominence on its low-wavenumber edge. This band(s), as well as those at higher wavenumber, are likely to have considerable charge-transfer character.

Upon reduction of the complex ions $[Fe_3O(O_2CMe)_6L_3]^+$ and $[Fe_3O(O_2CR)_6(py)_3]^+$ in the presence of free py or L an extremely broad (full width at half height ≈5000 cm^{-1}), weak band ($\varepsilon \approx 60$–100 dm^3 mol^{-1} cm^{-1}) is observed to grow in the region 7000–10 000 cm^{-1} which is attributed to an intervalence charge-transfer (IVCT) transition in a weakly interacting system.[1] The maximum of this transition does appear to vary somewhat with the identity of R and L but, given the broadness of the band, considerable uncertainty is associated with the determination of each absorption maximum. The growth of the IVCT band is accompanied by a general increase in absorbance across the visible region. The spectral changes occurring upon reduction of $[Fe_3O(O_2CMe)_6(4\text{-}NCpy)_3]^+$ are shown in Fig. 6. The growth of the various bands across the VIS/NIR region is accompanied by a decrease in intensity of the presumed charge-transfer transition at 28 500 cm^{-1}, with maintenance of an isosbestic point near 25 000 cm^{-1}. Upon completion of the electrolysis, reoxidation results in reformation of the starting spectrum, such that the reduction is chemically as well as voltammetrically reversible. However this was not the case for all of the triiron complexes; in some instances reduction was accompanied by non-isosbestic spectral changes, after which reoxidation did not yield the starting spectrum. For those complexes where the neutral mixed-valence species was electrogenerated successfully, *viz.* $[Fe_3O(O_2CMe)_6L_3]$ or $[Fe_3O(O_2CR)_6(py)_3]$, further reduction at the potential of the second process led to decomposition as judged by the non-isosbestic collapse of spectral features and the failure to regain the starting spectrum upon reoxidation. This result is consistent with the chemically irreversible voltammetry.

In the case of $R = CH_2CN$, where chemically reversible processes were observed on the voltammetric timescale, the $[Fe_3O(O_2CCH_2CN)_6(py)_3]^{+/0}$ reduction was found to be irreversible on the spectroelectrochemical timescale, prohibiting characterisation of the mixed-valence $[Fe_3O(O_2CCH_2CN)_6(py)_3]$ {and therefore $[Fe_3O(O_2CCH_2CN)_6(py)_3]^-$} species. Unfortunately the complex was not sufficiently soluble at 213 K to permit low-temperature measurements.

Conclusion

The electrochemical and spectroelectrochemical studies described herein have shown that whilst the $[Fe_3O(O_2CR)_6L_3]^+$ complexes are readily reduced, the reduction products are not universally stable, particularly without the presence of an excess of py or substituted py. The stability of the reduced $[Fe_3O(O_2CR)_6L_3]$ species is dependent upon both the identity of the carboxylate functionality R and that of the neutral pyridine ligand L, and upon the presence of free pyridine. The ability to vary the $[Fe_3O(O_2CR)_6L_3]^{+/0}$ reduction potential through alteration of R and L provides a means of tuning the oxidising strength of the complex, which could be important since several $[Fe_3O(O_2CR)_6L_3]^+$ complexes (R = Me or Bu^t, L = H_2O or py) have previously been shown to be effective catalysts for the epoxidation of olefins.[41] The $[Fe_3O(O_2CCH_2CN)_6(py)_3]^+$ ion is, to the best of our knowledge, the only first-row $[M_3O(O_2CR)_6L_3]^+$ species to exhibit more than one, voltammetrically reversible, redox step. Whilst the $[Fe_3O(O_2CCH_2CN)_6(py)_3]$ and $[Fe_3O(O_2CCH_2CN)_6(py)_3]^-$ species are stable on the timescale of the voltammetric experiment, the reduction of $[Fe_3O(O_2CCH_2CN)_6(py)_3]^+$ is chemically irreversible on the spectroelectrochemical timescale at room temperature.

Acknowledgements

The authors thank the Ramsay Memorial Fellowships Trust for the award of a British Ramsay Fellowship (to D. G. H.) and Dr. Lesley Yellowlees and Dr. Ken Taylor (University of Edinburgh) for the use of facilities used to collect several of the electrogenerated UV/VIS/NIR spectra.

References

1 R. D. Cannon and R. P. White, *Prog. Inorg. Chem.*, 1988, **36**, 195.
2 J. Catterick and P. Thornton, *Adv. Inorg. Chem. Radiochem.*, 1977, **20**, 291.

3 (*a*) L. Meesuk, R. P. White, B. Templeton, U. A. Jayasooriya and R. D. Cannon, *Inorg. Chem.*, 1990, **29**, 2389; (*b*) O. Almog, A. Bino and D. Garfinkel-Shweky, *Inorg. Chim. Acta*, 1993, **213**, 99; (*c*) R. D. Cannon, U. A. Jayasooriya, L. Montri, A. K. Saad, E. Karu, S. K. Bollen, W. R. Sanderson, A. K. Powell and A. B. Blake, *J. Chem. Soc.*, *Dalton Trans.*, 1993, 2005; (*d*) A. Harton, M. K. Nagi, M. M. Glass, P. C. Junk, J. L. Atwood and J. B. Vincent, *Inorg. Chim. Acta*, 1994, **217**, 171; (*e*) M. Abe, Y. Sasaki, Y. Yamada, K. Tsukahara, S. Yano and T. Ito, *Inorg. Chem.*, 1995, **34**, 4490; (*f*) S. L. Castro, W. E. Streib, J. Sun and G. Christou, *Inorg. Chem.*, 1996, **35**, 4462; (*g*) J. P. Bourke, E. Karu and R. D. Cannon, *Inorg. Chem.*, 1996, **35**, 1577; (*h*) J. K. Beattie, T. W. Hambley, J. A. Klepetko, A. F. Masters and P. Turner, *Polyhedron*, 1996, **15**, 2141; (*i*) M. Velayutham, C. S. Gopinath and S. Subramanian, *Chem. Phys. Lett.*, 1996, **249**, 71.
4 B. N. Figgis and G. B. Robertson, *Nature* (*London*), 1965, **205**, 694.
5 D. N. Hendrickson, S. M. Oh, T. Dong, T. Kambara, M. J. Cohn and M. F. Moore, *Comments Inorg. Chem.*, 1985, **4**, 329; T. Nakamoto, M. Katada, S. Kawata, S. Kitagawa, K. Kikuchi, I. Ikemoto, K. Endo and H. Sano, *Chem. Lett.*, 1993, 1463; R. P. White, J. A. Stride, S. K. Bollen, N. C. Bollen, G. J. Kearley, U. A. Jayasooriya and R. D. Cannon, *J. Am. Chem. Soc.*, 1993, **115**, 7778; R. Wu, S. K. A. Koske, R. P. White, C. E. Anson, U. A. Jayasooriya and R. D. Cannon, *J. Chem. Soc.*, *Chem. Commun.*, 1994, 1657; K. Asamaki, T. Nakamoto, S. Kawata, H. Sano, M. Katada and K. Endo, *Inorg. Chim. Acta*, 1995, **236**, 155; T. Sato, F. Ambe, K. Endo, M. Katada, H. Maeda, T. Nakamoto and H. Sano, *J. Am. Chem. Soc.*, 1996, **118**, 3450; T. Nakamoto, M. Yoshida, S. Kitagawa, M. Katada, K. Endo and H. Sano, *Polyhedron*, 1996, **15**, 2131.
6 R. D. Cannon, U. A. Jayasooriya, R. Wu, S. K. Arapkoske, J. A. Stride, O. F. Nielsen, R. P. White, G. J. Kearley and D. Summerfield, *J. Am. Chem. Soc.*, 1994, **116**, 11 869.
7 A. B. Blake, A. Yavari, W. E. Hatfield and C. N. Sethulekshmi, *J. Chem. Soc.*, *Dalton Trans.*, 1985, 2509 and refs. therein.
8 (*a*) D. D. Perrin, *J. Chem. Soc.*, 1959, 1710; (*b*) L. Ciavatta, G. Nunziata and L. G. Sillén, *Acta Chem. Scand.*, 1969, **23**, 1637; (*c*) S. V. Kukharenko, V. V. Strelets and O. N. Efimov, *Sov. Electrochem.*, 1983, **19**, 1436; (*d*) ref. 1, p. 212; (*e*) R. D. Cannon, L. Montri, D. B. Brown, K. M. Marshall and C. M. Elliot, *J. Am. Chem. Soc.*, 1984, **106**, 2591; (*f*) K. Nakata, A. Nagasawa, Y. Sasaki and T. Ito, *Chem. Lett.*, 1989, 753; (*g*) R. P. White, L. M. Wilson, D. J. Williamson, G. R. Moore, U. A. Jayasooriya and R. D. Cannon, *Spectrochim. Acta*, *Part A*, 1990, **46**, 917; (*h*) R. Manchanda, *Inorg. Chim. Acta*, 1996, **245**, 91; (*i*) G. Losada, M. Antonia Mendolia and M. Teresa Sevilla, *Inorg. Chim. Acta*, 1997, **255**, 125.
9 C. T. Dziobkowski, J. T. Wrobleski and D. B. Brown, *Inorg. Chem.*, 1981, **20**, 671.
10 S. M. Oh, D. N. Hendrickson, K. L. Hassett and R. E. Davis, *J. Am. Chem. Soc.*, 1985, **107**, 8009.
11 A. Earnshaw, B. N. Figgis and J. Lewis, *J. Chem. Soc. A*, 1966, 1656.
12 G. J. Long, W. T. Robinson, W. P. Tappmeyer and D. L. Bridges, *J. Chem. Soc.*, *Dalton Trans.*, 1975, 573.
13 N. S. Gill, R. H. Nuttall, D. E. Scaife and D. W. A. Sharp, *J. Inorg. Nucl. Chem.*, 1961, **18**, 79.
14 R. J. H. Clark and D. G. Humphrey, *Inorg. Chem.*, 1996, **36**, 2053.
15 S. A. Macgregor, E. J. L. McInnes, R. J. Sorbie and L. J. Yellowlees, *Molecular Electrochemistry of Inorganic*, *Bioinorganic and Organometallic Complexes*, eds. A. J. L. Pombeiro and J. A. McCleverty, Kluwer Academic Publishers, Dordrecht, 1993, p. 503.
16 S. R. Hall, G. S. D. King and J. M. Stewart, *The Xtal 3.4 User's Manual*, The University of Western Australia, Lamb, Perth, 1995.
17 G. B. Deacon and R. J. Phillips, *Coord. Chem. Rev.*, 1980, **33**, 227.
18 A. R. Katritzky and A. P. Ambler, *Physical Methods in Heterocyclic Chemistry*, Academic Press, London, 1963, vol. 2, ch. 10, p. 161.
19 L. Montri and R. D. Cannon, *Spectrochim. Acta*, *Part A*, 1985, **41**, 643.
20 K. Nakamoto, *Infrared and Raman Spectra of Inorganic and Coordination Compounds*, Wiley-Interscience, New York, 4th edn., 1986, pp. 124, 138.
21 J. C. Daran, Y. Jeannin and L. M. Martin, *Inorg. Chem.*, 1980, **19**, 2935.
22 H. Y. Wang, W. J. Chen, C. C. Yang and A. Yeh, *Inorg. Chem.*, 1991, **30**, 1862.
23 A. B. Blake and L. S. Fraser, *J. Chem. Soc.*, *Dalton Trans.*, 1975, 193.
24 J. Catterick, P. Thornton and B. W. Fitzsimmons, *J. Chem. Soc.*, *Dalton Trans.*, 1977, 1420.
25 N. V. Gerbeleu, G. A. Timko, K. I. Turte, G. A. Popovich, S. A. Bobkova and K. M. Indrichan, *Russ. J. Inorg. Chem.*, 1986, **31**, 390.
26 E. Spinner, *J. Chem. Soc.*, 1964, 4217.
27 D. A. Thornton, *Coord. Chem. Rev.*, 1990, **104**, 251.
28 C. H. Kline and J. Yurkevich, *J. Chem. Phys.*, 1944, **12**, 300.
29 F. Degang, W. Guoxiong and T. Wenxia, *Polyhedron*, 1993, **12**, 2459.
30 V. M. Lynch, J. W. Sibert, J. L. Sessler and B. E. Davis, *Acta Crystallogr.*, *Sect. C*, 1991, **47**, 866.
31 (*a*) J. Heinze, *Angew. Chem.*, *Int. Ed. Engl.*, 1984, **23**, 831; (*b*) R. S. Nicholson, *Anal. Chem.*, 1966, **38**, 1406.
32 A. M. Bond and D. G. Humphrey, unpublished work.
33 (*a*) J. A. Baumann, D. J. Salmon, S. T. Wilson, T. J. Meyer and W. E. Hatfield, *Inorg. Chem.*, 1978, **17**, 3342; (*b*) H. E. Toma, C. J. Cunha and C. Cipriano, *Inorg. Chim. Acta*, 1988, **154**, 63; (*c*) K. Takahashi, K. Umakoshi, A. Kikuchi, Y. Sasaki, M. Tominaga and I. Taniguchi, *Z. Naturforsch.*, *Teil B*, 1995, **50**, 551; (*d*) M. Abe, Y. Sasaki, Y. Yamada, K. Tsukahara, S. Yano, T. Yamaguchi, M. Tominaga, I. Taniguchi and T. Ito, *Inorg. Chem.*, 1996, **35**, 6724.
34 J. March, *Advanced Organic Chemistry—Reactions*, *Mechanisms and Structure*, Wiley-Interscience, New York, 4th edn., 1992, p. 265.
35 N. A. Lange, *Lange's Handbook of Chemistry*, ed. J. A. Dean, McGraw-Hill, London, 14th edn., 1992, pp. 5–18.
36 N. S. Hush and R. J. M. Hobbs, *Prog. Inorg. Chem.*, 1968, **10**, 259.
37 A. B. P. Lever, *Inorganic Electronic Spectroscopy*, Elsevier, Amsterdam, 2nd edn., 1984, pp. 87–90, 453.
38 R. N. Puri, R. O. Asplund and S. L. Holt, *J. Coord. Chem.*, 1981, **11**, 125; R. N. Puri and R. O. Asplund, *Inorg. Chim. Acta*, 1981, **54**, L187; (*c*) N. Puri, R. O. Asplund and W. F. Tucker, *Inorg. Chim. Acta*, 1982, **66**, 7.
39 Ref. 37, p. 751.
40 L. Dubicki and R. L. Martin, *Aust. J. Chem.*, 1969, **22**, 701.
41 S. Ito, K. Inoue and M. Mastumoto, *J. Am. Chem. Soc.*, 1982, **104**, 6450.

Received 10*th December* 1997; *Paper* 7/08880I